AD-A092 057 AIR FORCE ENGINEERING AND SERVICES CENTER TYNDALL AF--ETC F/G 1/3
MODAL ANALYSIS FOR AIRCRAFT RESPONSE TO RUNWAY SURFACE ROUGHNES--ETC(U)
JUN 80 R R GAJEWSKI

UNCLASSIFIED AFESC/ESL-TR-80-32 NL

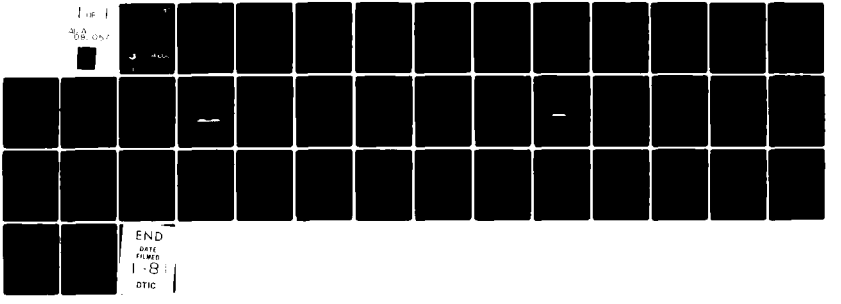

END
DATE FILMED
1-81
DTIC

LEVEL II

ESL-TR-80-32

MODAL ANALYSIS FOR AIRCRAFT RESPONSE TO RUNWAY SURFACE ROUGHNESS

RALPH R. GAJEWSKI, CAPT, USAF
DEPARTMENT OF ENGINEERING MECHANICS
UNITED STATES AIR FORCE ACADEMY
COLORADO 80840

JUNE 1980

FINAL REPORT
1 JUNE 1978 — 30 JUNE 1980

APPROVED FOR PUBLIC RELEASE: DISTRIBUTION UNLIMITED

AFESC

ENGINEERING & SERVICES LABORATORY
AIR FORCE ENGINEERING & SERVICES CENTER
TYNDALL AIR FORCE BASE, FLORIDA 32403

NOTICE

Please do not request copies of this report from HQ AFESC/RD (Engineering and Services Laboratory). Additional copies may be purchased from:

National Technical Information Service
5285 Port Royal Road
Springfield, Virginia 22161

Federal Government agencies and their contractors registered with Defense Technical Information Center should direct requests for copies of this report to:

Defense Technical Information Center
Cameron Station
Alexandria, Virginia 22314

UNCLASSIFIED

SECURITY CLASSIFICATION OF THIS PAGE (When Data Entered)

REPORT DOCUMENTATION PAGE	READ INSTRUCTIONS BEFORE COMPLETING FORM
1. REPORT NUMBER: ESL-TR-80-32	2. GOVT ACCESSION NO.: AD-A092 057
	3. RECIPIENT'S CATALOG NUMBER
4. TITLE (and Subtitle): MODAL ANALYSIS FOR AIRCRAFT RESPONSE TO RUNWAY SURFACE ROUGHNESS	5. TYPE OF REPORT & PERIOD COVERED: Final Report, June 1978 - June 1980
	6. PERFORMING ORG. REPORT NUMBER
7. AUTHOR(s): Ralph R. Gajewski, Capt, USAF	8. CONTRACT OR GRANT NUMBER(s)
9. PERFORMING ORGANIZATION NAME AND ADDRESS: Department of Engineering Mechanics, United States Air Force Academy, Colorado 80840	10. PROGRAM ELEMENT, PROJECT, TASK AREA & WORK UNIT NUMBERS: PE: 63723F, JON: 2104-2B-30
11. CONTROLLING OFFICE NAME AND ADDRESS: Air Force Engineering and Services Center, Tyndall Air Force Base, FL 32403	12. REPORT DATE: June 1980
	13. NUMBER OF PAGES: 40
14. MONITORING AGENCY NAME & ADDRESS (if different from Controlling Office)	15. SECURITY CLASS. (of this report): Unclassified
	15a. DECLASSIFICATION/DOWNGRADING SCHEDULE

16. DISTRIBUTION STATEMENT (of this Report)

Approved for public release; distribution unlimited.

17. DISTRIBUTION STATEMENT (of the abstract entered in Block 20, if different from Report)

18. SUPPLEMENTARY NOTES

Availability of this report is specified on verso of front cover.

19. KEY WORDS (Continue on reverse side if necessary and identify by block number)

F-4E TAXI Tests
Runway Roughness
AM-2 Mats
Rapid Runway Repair
Modal Analysis

20. ABSTRACT (Continue on reverse side if necessary and identify by block number)

This report develops one and three degree-of-freedom linear vibration models for the prediction of aircraft response to runway surface roughness. The equations of motion are integrated in principal coordinates using modal analysis. The modal parameters required are natural frequency, damping ratio, and mode shape for each degree of freedom. Comparison of results is made with the TAXI code that has a nonlinear strut model. Results are presented for asymmetric motion due to spall profiles in the runway.

DD FORM 1 JAN 73 1473 EDITION OF 1 NOV 65 IS OBSOLETE

UNCLASSIFIED

SECURITY CLASSIFICATION OF THIS PAGE (When Data Entered)

PREFACE

This report was prepared by the Department of Engineering Mechanics, United States Air Force Academy, Colorado, 80840, for the Engineering and Services Laboratory at Tyndall AFB, Florida, under Job Order Number 21042B30 during the period June 1978 through June 1980. The Project Officer was Capt David Salz, AFESC/RDCR.

This report has been reviewed by the Public Affairs Office (PA) and is releasable to the National Technical Information Service (NTIS). At NTIS, it will be available to the general public including foreign nationals.

This technical report has been reviewed and is approved for publication.

DAVID SALZ, Capt, USAF
Project Officer

LAPSLEY R. CALDWELL, Lt Col, USAF
HAVE BOUNCE Program Manager

ROBERT E. BOYER, Lt Col, USAF
Chief, Engineering Research Division

FRANCIS B. CROWLEY III, Colonel, USAF
Dir, Engineering & Services Laboratory

Accession For	
NTIS GRA&I	X
DTIC TAB	☐
Unannounced	☐
Justification	
By	
Distribution/	
Availability Codes	
Dist	Avail and/or Special
A	

(The reverse of this page is blank)

TABLE OF CONTENTS

Section	Title	Page
I	INTRODUCTION	1
II	EQUATIONS OF MOTION	2
III	SOLUTIONS	8
IV	RESULTS	12
V	CONCLUSIONS AND RECOMMENDATIONS	32

LIST OF FIGURES

Figure	Title	Page
1	Aircraft Geometry and Coordinates	3
2	Piecewise Linear Runway Profile	8
3	Half Mat Profile	14
4	TAXI Results for Half Mat Profile	16
5	SDOF Results for Half Mat Profile	17
6	3DOF Results for Half Mat Profile	18
7	Full Mat Profile	19
8	TAXI Code Response to Full Mat Profile	20
9	SDOF Code Response to Full Mat Profile	21
10	3DOF Code Response to Full Mat Profile	22
11	SDOF Code Response with Frequency = 1.80 Hertz	23
12	3DOF Code Response with Modified Spring Constants	24
13	Spall Models	25
14	Response to Two Foot Spall for Left Main Gear Input	26
15	Response to Two Foot Spall for Left Main and Nose Gear Input	27
16	Response to Two Foot Spall for Three Gear Input	28
17	Response to Double Spall for Left Main Gear Input	29
18	Response to Double Spall for Left Main and Nose Gear Input	30
19	Response to Double Spall for Three Gear Input	31

LIST OF TABLES

Table	Title	Page
1	Aircraft Model Data	12
2	Equivalent Spring Stiffness	12
3	Mode Shapes and Frequencies	13
4	Revised Mode Shapes and Frequencies	15

(The reverse of this page is blank)

SECTION I

INTRODUCTION

The United States Air Force requires the capability to operate aircraft on rough runways created by the rapid repair of bomb damage (Reference 1). The current rapid runway repair technique uses AM-2 matting and procedures described in Air Force Regulation 93-2 (Reference 2). Initial data for F-4E performance on AM-2 mats have been acquired in the HAVE BOUNCE test program (References 3 and 4). These data can also be used to validate computer simulations of aircraft response to runway surface roughness. These computer simulations may then be used to develop surface roughness criteria (Reference 5).

The United States Air Force Academy (USAFA) has provided engineering consultation on surface roughness to the Air Force Engineering and Services Center (AFESC) since 1977. During this reporting period, evaluations have been provided for using statistical analysis techniques and using a stationary test facility for surface roughness evaluations. The purpose of this report is to develop a three-degree-of-freedom model for analysis of aircraft taxi response over repair mats and spalls. A one-degree-of-freedom model was used to predict the symmetric motion response for the HAVE BOUNCE Phase II program (Appendix C, Reference 4).

This report uses modal analysis to predict aircraft response to surface roughness. The rigid body aircraft model includes the bounce, pitch, and roll degrees of freedom. The surface roughness for the nose and two main gear tracks is modeled as a sequence of straight line segments, such as ramps and mats, placed on an originally flat runway surface. The equations of motion are integrated using modal superposition and the piecewise exact solution algorithm (Reference 6). The model will accept experimentally determined natural frequencies, damping ratios, and mode shapes. The modal superposition solution is suitable for programming on minicomputers. The results presented include a comparison with the TAXI computer code (Reference 7) and predictions of asymmetric motion due to spalls in the runway surface.

SECTION II

EQUATIONS OF MOTION

1. GEOMETRY. The aircraft model geometry and coordinates are shown in Figure 1. The spring and damping constants represent the strut and tire combined in series for vibrations about the equilibrium position. The attachment point displacements are kinematically related to the center of gravity displacements through a geometry matrix:

$$\{u_{NLR}\} = [GEOM]\{u_G\} \tag{1}$$

where

$$\{u_{NLR}\} = \begin{Bmatrix} u_N \\ u_L \\ u_R \end{Bmatrix}$$

$$[GEOM] = \begin{bmatrix} 1 & D_N & 0 \\ 1 & -D_M & D_L \\ 1 & -D_M & -D_R \end{bmatrix}$$

$$\{u_G\} = \begin{Bmatrix} u_{CG} \\ \theta \\ \phi \end{Bmatrix}$$

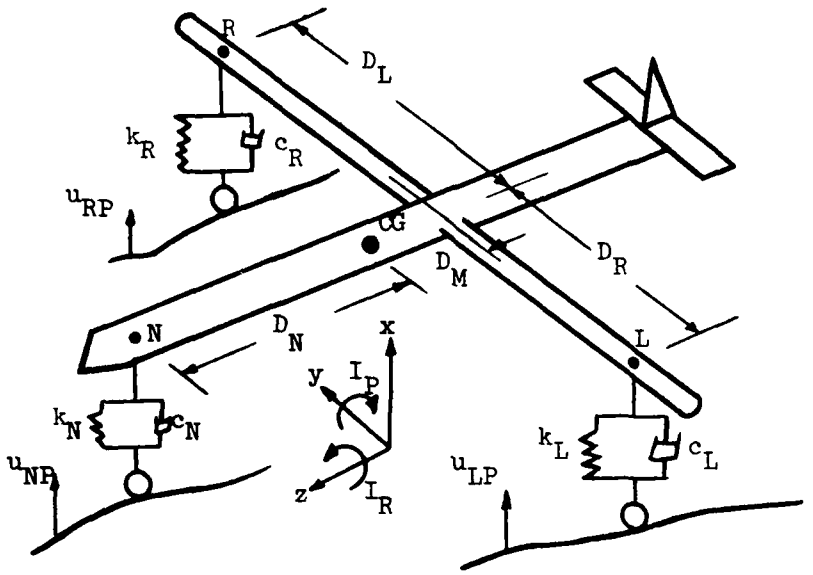

Figure 1. Aircraft Geometry and Coordinates

CG	Aircraft center of gravity
R,L,N	Strut attachment points for right main, left main, and nose gears
D_M, D_N	Moment arms from aircraft centerline
u_{RP}, u_{LP}, u_{NP}	Runway profiles for three gears, + upward
u_{CG}	Displacement of CG, + upward
θ	Pitch angle, + nose up
ϕ	Roll angle, + left wing up
M_{CG}, I_P, I_R	Mass, pitch and roll inertia
u_R, u_L, u_N	Displacement of attachment points, + upward
k_R, k_L, k_N	Gear spring constants
c_R, c_L, c_N	Gear damping constants

2. EQUATIONS OF MOTION. The equations of motion are derived assuming nose profile and attachment point displacements are ordered so that

$$u_{NP} > u_N > 0$$

and their slopes are ordered so that

$$\dot{u}_{NP} > \dot{u}_P > 0.$$

Then the total upward nose strut force acting on the aircraft is

$$F_{SN} = k_N (u_{NP} - u_N) + c_N (\dot{u}_{NP} - \dot{u}_N). \tag{2a}$$

Similarly, the upward main gear strut forces are

$$F_{SR} = k_R (u_{RP} - u_R) + c_R (\dot{u}_{RP} - \dot{u}_R) \tag{2b}$$

$$F_{SL} = k_L (u_{LP} - u_L) + c_L (\dot{u}_{LP} - \dot{u}_L) \tag{2c}$$

The equations of motion from summing forces vertically and summing moments about the pitch and roll axes are

$$\begin{aligned} F_{SN} + F_{SR} + F_{SL} &= M_{CG} \ddot{u}_{CG} \\ D_N F_{SN} - D_M (F_{SR} + F_{SL}) &= I_P \ddot{\theta} \\ D_L F_{SL} - D_R F_{SR} &= I_R \ddot{\phi} \end{aligned} \tag{3}$$

Define

$$[M] = \begin{bmatrix} M_{CG} & 0 & 0 \\ 0 & I_P & 0 \\ 0 & 0 & I_R \end{bmatrix}$$

These equations can be written in matrix form as

$$[M]\{\ddot{u}_G\} + [C_1]\{\dot{u}_{NLR}\} + [K_1]\{u_{NLR}\} = [K_1]\{u_P\} + [C_1]\{\dot{u}_P\} \tag{4}$$

where

$$\{u_P\} = \begin{Bmatrix} u_{PN} \\ u_{PL} \\ u_{PR} \end{Bmatrix}$$

$$[K_1] = [GEOM]^T \begin{bmatrix} k_N & 0 & 0 \\ 0 & k_L & 0 \\ 0 & 0 & k_R \end{bmatrix}$$

$$[C_1] = [GEOM]^T \begin{bmatrix} c_N & 0 & 0 \\ 0 & c_L & 0 \\ 0 & 0 & c_R \end{bmatrix}$$

Then using Equation (1) the left-hand side of Equation(4)can be re-written in center-of-gravity displacements as

$$[M]\{\ddot{u}_G\} + [C_D]\{\dot{u}_G\} + [K_D]\{u_G\} = [K_1]\{u_P\} + [C_1]\{\dot{u}_P\} \tag{5}$$

where

$$[K_D] = [GEOM]^T \begin{bmatrix} k_N & 0 & 0 \\ 0 & k_L & 0 \\ 0 & 0 & k_R \end{bmatrix} [GEOM]$$

$$[C_D] = [GEOM]^T \begin{bmatrix} c_N & 0 & 0 \\ 0 & c_L & 0 \\ 0 & 0 & c_R \end{bmatrix} [GEOM] .$$

3. MODAL EQUATIONS. The modal equations of motion are derived using the natural frequencies and mode shapes for the undamped system which are computed from standard vibrations techniques as in Reference 8 or computer techniques as in Reference 9. The system characteristic matrix equations are

$$\left([K_D] - \omega_i^2 [M]\right)\{MODE_i\} = \{0\} \tag{6}$$

where ω_i is the natural frequency and $\{MODE_i\}$ is the corresponding mode shape. Let [MODAL] be the modal matrix constructed using the mode shapes as columns. The mode shapes are orthonormalized so that

$$[MODAL]^T[M][MODAL] = [I] \tag{7}$$

where [I] is the identity matrix. Then

$$[MODAL]^T[K_D][MODAL] = [\omega_i^2] \tag{8}$$

is a diagonal matrix with the square of the natural frequencies on the diagonals.

The same sequence of matrix products does not generally diagonalize the damping matrix

$$[MODAL]^T[C_D][MODAL] = [C_p] \tag{9}$$

It is very desirable that a diagonal matrix $[C_p]$ be obtained so that the equations of motion will decouple with the introduction of principal coordinates {p} defined by

$$\{u_G\} = [MODAL]\{p\} \tag{10}$$

For lightly damped systems such as seen in the HAVE BOUNCE Phase I test results (Reference 3), it is reasonable to neglect the coupling of modes through the off-diagonal terms of $[C_p]$ and retain only the diagonal terms (Reference 6). These diagonal terms are then rewritten as

$$c_{pii} = 2\,\zeta_i\,\omega_i \tag{11}$$

where ζ_i is the ratio of damping in mode i to the critical damping for that mode.

The decoupled modal equations of motion are obtained through multiplying Equation(5)by $[MODAL]^T$ and substituting Equation(10),resulting in the sequence of equations of the form

$$\ddot{p}_i + 2\zeta_i \omega_i \dot{p}_i + \omega_i^2 p_i = \{MODE_i\}^T([K_1]\{u_p\} + [C_1]\{\dot{u}_p\}) \qquad (12)$$

Thus, the response of each mode can be solved as a single degree of freedom system and the total response found by superposition of the principal coordinate responses using Equation(10).

SECTION III

SOLUTIONS

1. DIRECT INTEGRATION. There are several methods for directly integrating the linear matrix equations of motion [Equation 5] such as the Newmark Method and Wilson θ Method (References 6 and 9). Some of these methods are conditionally stable, and each requires a small time step to minimize period elongation and amplitude decay of the results.

2. MODAL SUPERPOSITION. This method integrates the decoupled equations of motion [Equation(12)] separately and then adds each modal response for the total solution. If a direct integration method such as the Wilson θ Method with the same time step for all modes is used, the results will be the same as directly integrating the system matrix equations. But modal superposition provides the opportunity to only integrate the modal response for selected dominant modes and to use the accurate piecewise exact integration scheme which does not require a small time step for stability and accuracy as do the direct integration schemes.

3. PIECEWISE EXACT SOLUTION METHOD. Many types of loading, including the runway mat profile, can be closely approximated as a sequence of straight-line segments with unequal time intervals. For example, Figure 2 shows a runway mat profile with upheaval and settlement as constructed for the HAVE BOUNCE Phase II tests (Reference 4). Each straight-line segment, such as the second up-ramp illustrated in Figure 2, has its elevation written as a linear equation of the form $e_i(t) = a_i + b_i t$ where the subscript i denotes the segment number. The time axis values t are the product of multiplying the runway distance x and the constant ground speed of the aircraft V.

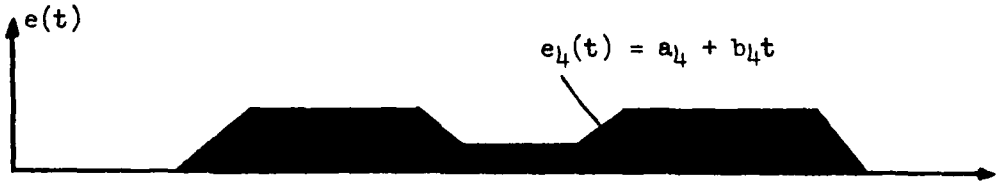

$$a_4 = e(t_s), \quad b_4 = \frac{e(t_f) - e(t_s)}{t_f - t_s}$$

Figure 2. Piecewise Linear Runway Profile

For any segment of time $t_s < t < t_f$, the one-dimensional vibration equation to be integrated is

$$\ddot{x} + 2\zeta\omega\dot{x} + \omega^2 x = \omega^2(a + bt) = A + Bt \qquad (13)$$

where a + bt is the equation for the mat profile in this time interval. The

exact displacement solution to Equation(13)is (Reference 6)

$$x(t) = A_0 + A_1 + A_2 e^{-\zeta \omega t} \cos \omega_d t + A_3 e^{-\zeta \omega t} \sin \omega_d t \qquad (14)$$

where

$$A_0 = \frac{A}{\omega^2} - \frac{2 \zeta_B}{\omega^3}$$

$$A_1 = \frac{B}{\omega^2}$$

$$A_2 = x(t_0) - A_0$$

$$A_3 = \frac{1}{\omega_d} (\dot{x}(t_0) + \zeta \omega A_2 - A_1)$$

$$\omega_d = \omega \sqrt{1 - \zeta^2}$$

The solution is exact so using a small time step for stability and accuracy is not required.

4. ONE-DIMENSIONAL MODAL ANALYSIS. The HAVE BOUNCE Phase I test results indicate the aircraft responds in a dominant bounce mode which is lightly damped (Reference 3). Based on these results, it appears that a single degree of freedom solution based on Equation(14)would give good estimates for main gear compression loads. The one-dimensional equation of motion is

$$\ddot{u} + 2 \zeta \omega \dot{u} + \omega^2 u = \omega^2 u_M(t) + 2 \zeta \omega \dot{u}_M(t) \qquad (15)$$

where $u_M(t)$ is the main gear track profile. The frequency ω and damping factor ζ may be obtained experimentally from a power spectral density analysis. The second term on the right-hand side of Equation(15)may be neglected due to the small amount of damping in the system. The main gear compression load is the sum of the dynamic forces and the weight (W).

$$F_M = M_{CG} \omega^2 (u_M(t) - u(t)) + M_{CG} 2 \zeta \omega (\dot{u}_M(t) - \dot{u}(t)) + W \qquad (16)$$

For lightly damped systems, the second term may be neglected and the resulting F_M will be a conservative estimate of the gear load.

This model has been programmed at the Air Force Flight Test Center (AFFTC) and shows good correlation with the HAVE BOUNCE Phase II test results (Reference 4).

5. THREE-DIMENSIONAL MODAL ANALYSIS. The success of the one-dimensional model indicates that a three-dimensional model could provide good results for the bounce, pitch, and roll degrees of freedom. This model would estimate nose gear forces as well as compute asymmetric roll response.

The modal analysis is based on integrating Equation (13) using Equation (14) for each mode and each gear track profile. For three modes and three tracks, this solution will require integrating Equation (14) up to nine separate times and adding the results.

Since Equation (14) is being integrated in principal coordinates, the gear loads are not entered directly. Instead, the gear loads are partitioned using the mode shape vector. This partitioning accounts for how much the gear load is exciting a particular mode shape.

For example, consider the modal solution due to left main gear profile only. The gear load is partitioned using the orthonormalized mode shapes that satisfy Equation (7). The first modal equation is

$$\ddot{p}_1(t) + 2\,\zeta_1\omega_1\,\dot{p}_1(t) + \omega_1^2\,p_1(t) = P_{L_1}(t) \tag{17}$$

where the load participation is

$$P_{L_1}(t) = \{MODE_1\}^T[K_1] \begin{Bmatrix} 0 \\ u_{LP}(t) \\ 0 \end{Bmatrix} \tag{18}$$

For each segment of time where $P_{L_1}(t) = A + Bt$, the solution for $p_1(t)$ is found using Equation (14) with $\omega = \omega_1$. The load participation for the other modes is found using the appropriate mode shape in Equation (18) and the response found using the appropriate frequency and damping factor in Equation (14). The center-of-gravity displacements are found using the modal matrix

$$\begin{Bmatrix} u_{CG} \\ \theta \\ \phi \end{Bmatrix} = [MODAL] \begin{Bmatrix} p_1 \\ p_2 \\ p_3 \end{Bmatrix} \tag{19}$$

and the attachment point displacements are found using the geometry matrix

$$\begin{Bmatrix} u_N \\ u_L \\ u_R \end{Bmatrix} = [GEOM] \begin{Bmatrix} u_{CG} \\ \theta \\ \phi \end{Bmatrix} \tag{20}$$

The gear compression loads are computed using

$$F_N = -k_N u_N + F_{NST}$$

$$F_L = -k_L (u_L - u_{LP}) + F_{MST} \qquad (21)$$

$$F_R = -k_R u_R + F_{MST}$$

where F_{NST} and F_{MST} are nose and main gear static loads. The response for the nose and right main tracks follow in a similar manner.

SECTION IV

RESULTS

Calculational results for the single-degree-of-freedom model (SDOF) and the three-degree-of-freedom model (3DOF) will be compared with results from the TAXI computer code (Reference 7). Then spall results using the 3DOF model will be presented.

1. TAXI CODE. This code was provided by the Air Force Wright Aeronautical Laboratory (AFWAL). Additional FORTRAN coding was added to interface with the USAFA computer plotting system and to evaluate slope of the strut air curve formulas to obtain spring constants for the linear vibrations model.

2. COMPARISON MODEL. The heavy-weight aircraft data of Table 1 was obtained from AFFTC. The initial spring constants for the vibrations models were obtained from the TAXI code by computing the slope of the strut air curve at the static equilibrium position. This slope gives an overall stiffness for the strut which is then added to the tire stiffness in series (Reference 8) to obtain an overall gear stiffness.

TABLE 1. AIRCRAFT MODEL DATA

M_{CG}	=	145.5 lb·sec^2/in
I_P	=	1.92(10^6) lb·sec^2·in
I_R	=	6.56(10^5) lb·sec^2·in
$D_L = D_R$	=	109.25 in
D_N	=	234.9 in
D_M	=	44.35 in

TABLE 2. EQUIVALENT SPRING STIFFNESS

Main Gear	
Strut Stiffness	27809 lb/in
Tire Stiffness	13530 lb/in
Series Stiffness	9102 lb/in
Nose Gear	
Strut Stiffness	1662 lb/in
Tire Stiffness	15600 lb/in
Series Stiffness	1502 lb/in

3. THREE-DEGREE-OF-FREEDOM (3DOF) MODEL. The linear vibrations model for the data of Tables 1 and 2 has the mode shapes and frequencies shown in Table 3.

TABLE 3. MODE SHAPES AND FREQUENCIES

	Mode 1	Mode 2	Mode 3
ω	7.271 rad/s	12.016 rad/s	18.198 rad/s
x_g	0.025931	-0.078743	0
θ	0.000685	0.000226	0
ϕ	0	0	0.001235

The mode shapes indicate relative motion within a mode and are orthonormalized according to Equation (7). The first mode has its node 37.9 inches aft of the CG so its primary motion is pitching at the nose gear. The second mode has its node 348.4 inches forward of the CG so its primary motion is bouncing. The third mode is the roll mode which is decoupled from the bounce and pitch modes due to symmetry of the aircraft.

4. SINGLE-DEGREE-OF-FREEDOM (SDOF) MODEL. This model is based on the bounce mode so it uses ω = 12.016 rad/s and M = 145.5 sec^2/in. Both SDOF and 3DOF models were programmed using CAL (References 6 and 10), a computer analysis language developed for educational use at the University of California at Berkeley. The basic programming of Equation (14) is simple and can be done in almost any computer language.

5. RESPONSE TO HALF MAT PROFILE. The half mat profile used for the following calculations is shown in Figure 3. The TAXI code response for a constant velocity of 20 knots is shown in Figure 4. The frequency of vibration after coming off the mat is 1.80 Hertz, and the ratio of damping to critical damping is about 1%.

The SDOF response for a natural bounce mode frequency of 1.91 Hertz (Mode 2) and damping factor of 1 percent is shown in Figure 5. The straight line through the plot is the static equilibrium load. The maximum compression load is slightly larger than the TAXI response, but the minimum values are much smaller including unloading at the fourth minimum.

The 3DOF response for a 20-knot constant run with 1 percent damping in all three modes is shown in Figure 6. The straight lines through the plots are static equilibrium values. The maximum main gear compression loads are slightly smaller than both the TAXI and SDOF results, and the minimum values lie in between the other two runs. The nose gear response is smaller to the TAXI response but does not contain the highest frequency motion.

6. RESPONSE TO FULL MAT PROFILE. The full mat profile used for the following calculations is shown in Figure 7. The TAXI code response for a 20-knot run is shown in Figure 8. The main gear compression load coming off the mat (at three seconds on the figure) shows a reduction of the amplitude of vibration. A comparison of the TAXI code responses of Figures 4 and 8 indicates that the trailing edge of the mat can cause reinforcement or cancellation of the motion. To obtain accurate simulations of experimental results showing such reinforcements and cancellations, the computer model must have the same period of vibration in its dominant mode as the aircraft.

The SDOF response for a frequency of 1.91 Hertz and damping factor of 1 percent in shown in Figure 9. The initial response coming on the mat is similar to the TAXI response, but the linearized frequency of 1.91 Hertz causes the phasing of the trailing edge of the mat so that the motion is amplified.

The 3DOF response for a 20-knot run with 1 percent damping in all three modes is shown in Figure 10. The main gear response is very similar to the SDOF response showing an amplification at the end of the mat. The nose gear response is very similar to that for the TAXI code response.

The difference in phasing at the end of the mat is due to a different effective frequency of vibration about the equilibrium position. The SDOF and 3DOF results used the slope of the air curve at equilibrium as a component value to compute the series stiffness of the gear assembly. The TAXI code uses a nonlinear model for the compression air curve behavior of the strut as well as nonlinear damping.

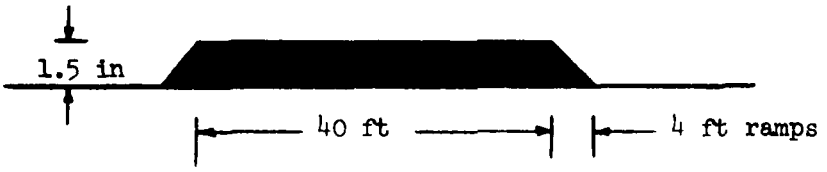

Figure 3. Half Mat Profile

To evaluate the effects of the nonlinear TAXI model, the effective spring constant, the change in pneumatic force divided by the change in strut compression was computed for each output value. The main gear spring constant ranges from a low of 4733 lb/in to a high of 11,362 lb/in. The nose gear spring constant ranges from a low of 965 lb/in to a high of 2662 lb/in. This variation in spring constants should be averaged in such a way that the equivalent spring constant yields the same period of free vibration while the aircraft is on the mat. Since the period is inversely proportional to the square root of the spring constant, it is reasonable to compute the equivalent spring constant according to

$$\frac{1}{\sqrt{k_{eq}}} = \frac{1}{n} \sum_{i=1}^{n} \frac{1}{\sqrt{k_i}} \qquad (22)$$

The revised spring constants are 8081 lb/in. for the main gear and 1508 lb/in for the nose gear. The revised mode shapes and frequencies are shown in Table 4.

TABLE 4. REVISED MODE SHAPES AND FREQUENCIES

	Mode 1	Mode 2	Mode 3
ω	7.282	11.328	17.148
x_g	0.025052	-0.079027	0
θ	0.000688	0.000218	0
ϕ	0	0	0.001235

The bounce mode frequency is now 1.80 Hertz. The SDOF results using this fundamental frequency are shown in Figure 11. The 3DOF results using the revised mode shapes and frequencies of Table 4 are shown in Figure 12. Figures 11 and 12 now show much better agreement with the TAXI code results of Figure 8. In particular, the cancellation of motion at the trailing edge of the mat is consistent for each calculation.

7. SPALL MODEL RESULTS. The spall profiles used for the following calculations are shown in Figure 13. These profiles correspond to the spalls cut into the runway for testing at AFFTC. The spalls were cut across the runway so that tests could be made with the left main gear only entering the spall and other tests could be made with both the nose gear and left main gear entering the same spall profile.

Figure 14 shows the response for the left main gear entering the two-foot spall with a speed of 10 knots. Figure 15 shows the response for the nose gear and left main gear entering the two-foot spall cut across the runway with a speed of 10 knots. Figure 16 shows the symmetrical response for all three gears entering the two-foot spall. The main gear compression loads are of about the same magnitude as shown for the mat encounters. The maximum left main gear compression load is larger for the asymmetric spall input (Figure 15) than for the symmetric spall input (Figure 16).

Figure 17 shows the response for the left main gear entering the double spall with a speed of 10 knots. Figure 18 shows the response for the nose gear and left main gear entering the double spall cut across the runway. Figure 19 shows the response for all three gears entering the double spall. The sharp downward plunge of the main gear compression follows from the assumption that the gear follows the runway profile. The effect of the tire footprint following such a spall profile is not included in these results but may be added by modifying the runway profile input. The maximum main gear compression load is larger for the asymmetric input (Figure 18) than for the symmetric input (Figure 19).

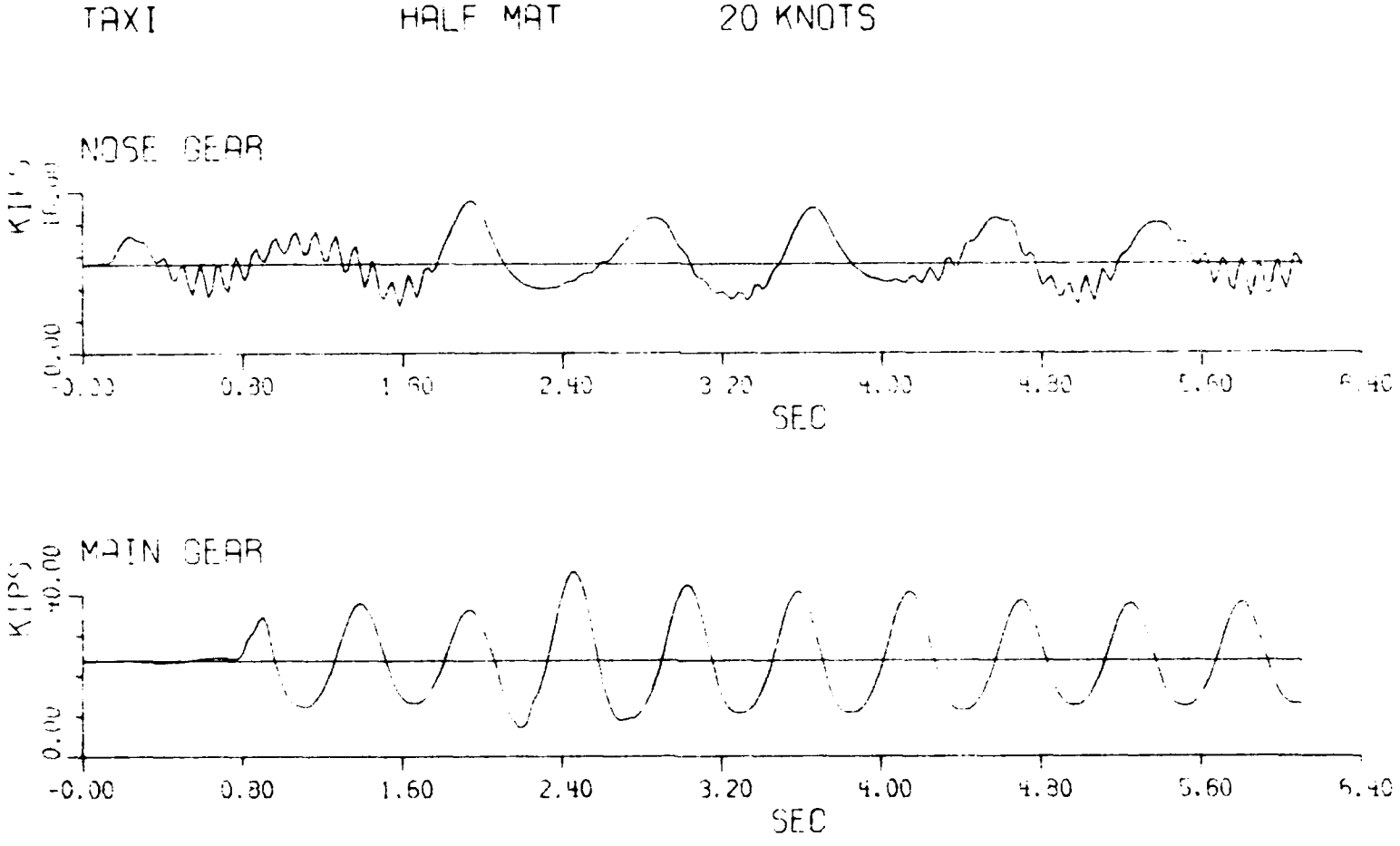

Figure 4. TAXI Code Response to Half Mat Profile

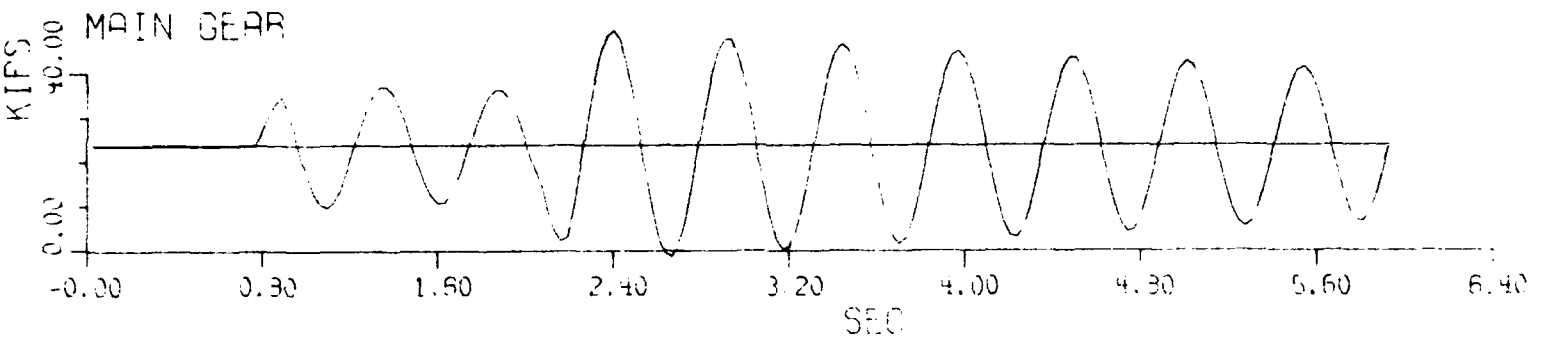

Figure 5. SDOF Code Response to Half Mat Profile

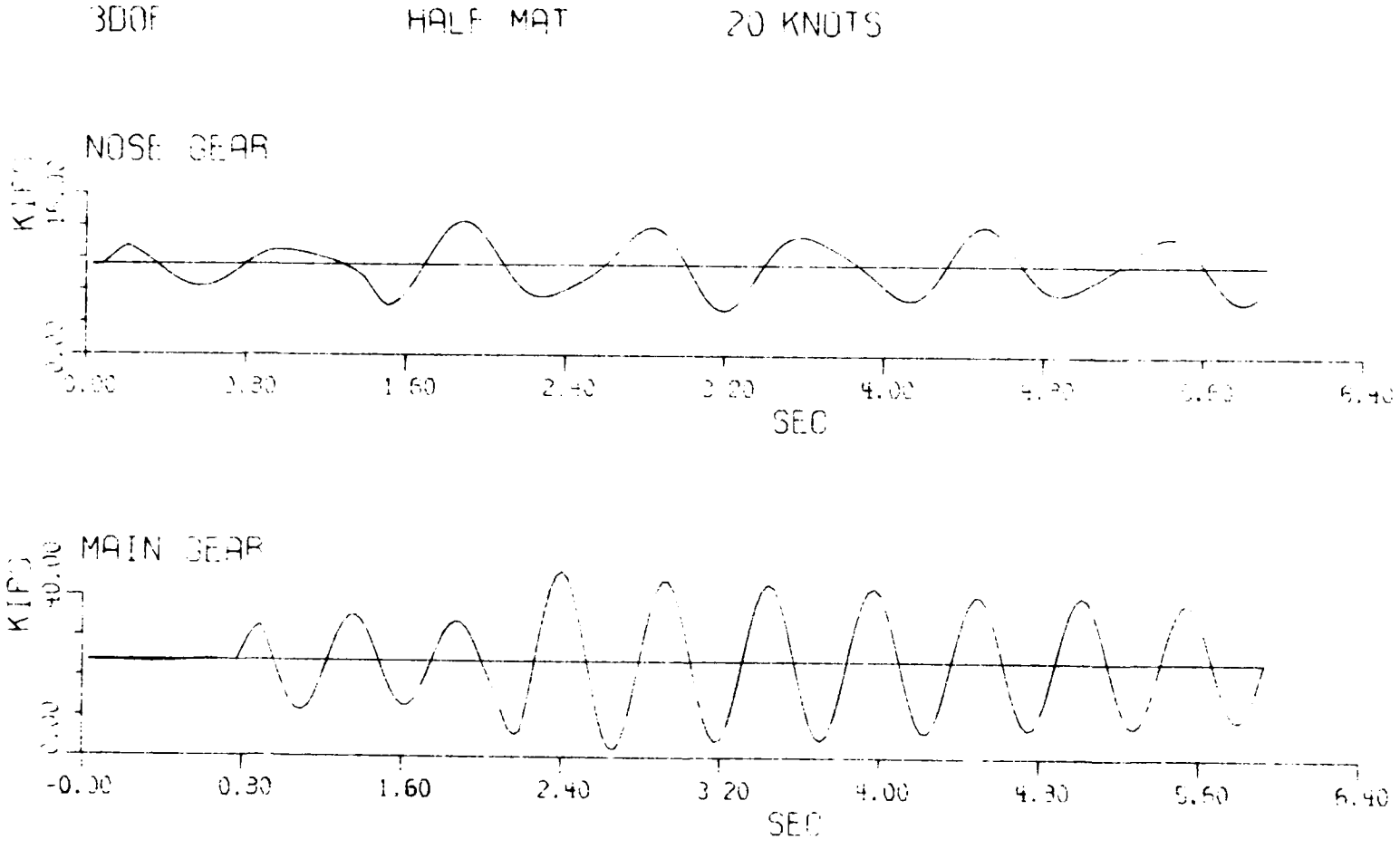

Figure 6. 3DOF Code Response to Half Mat Response

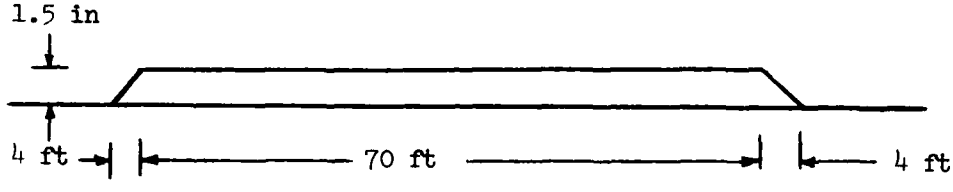

Figure 7. Full Mat Profile

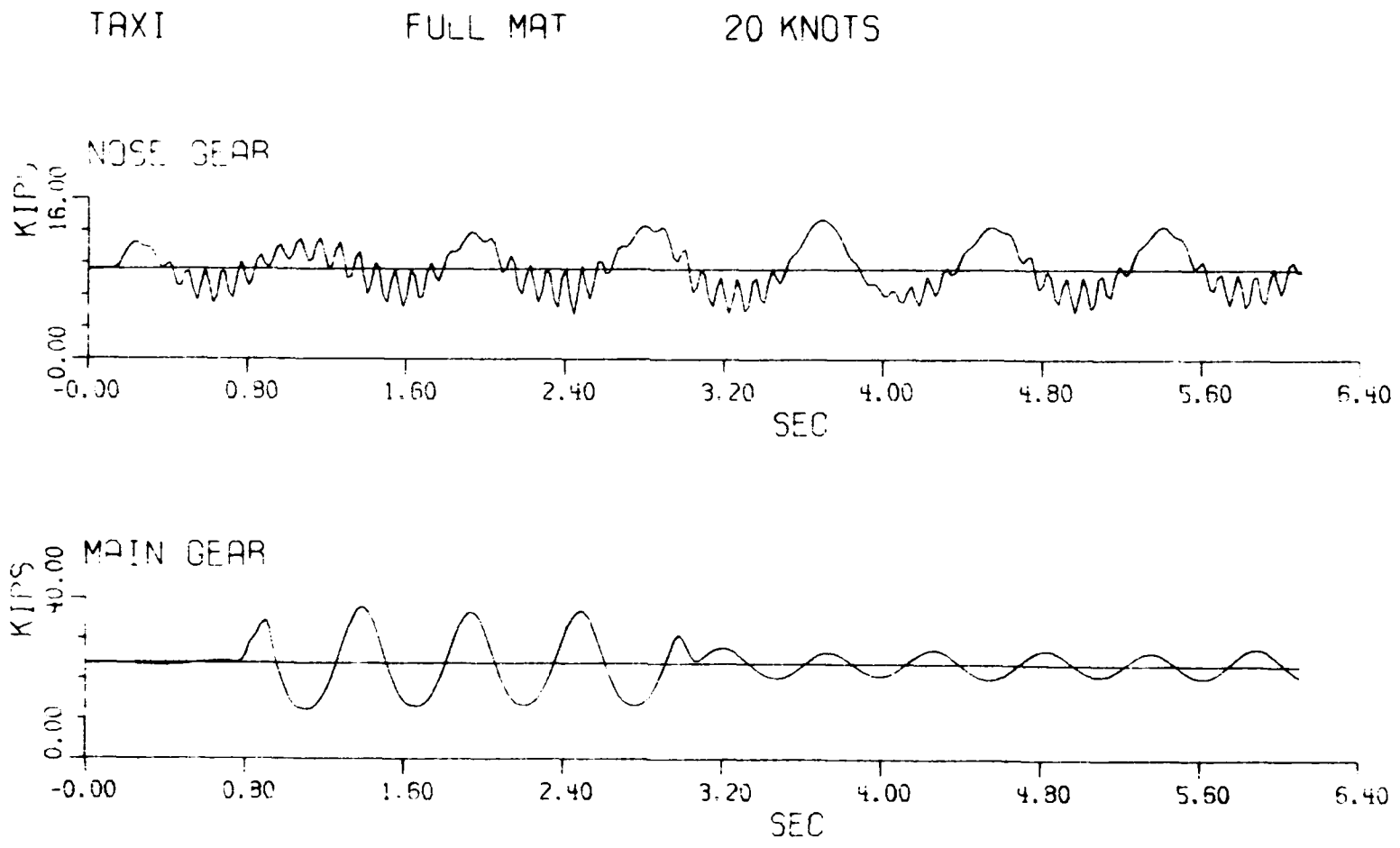

Figure 8. TAXI Code Response to Full Mat Profile

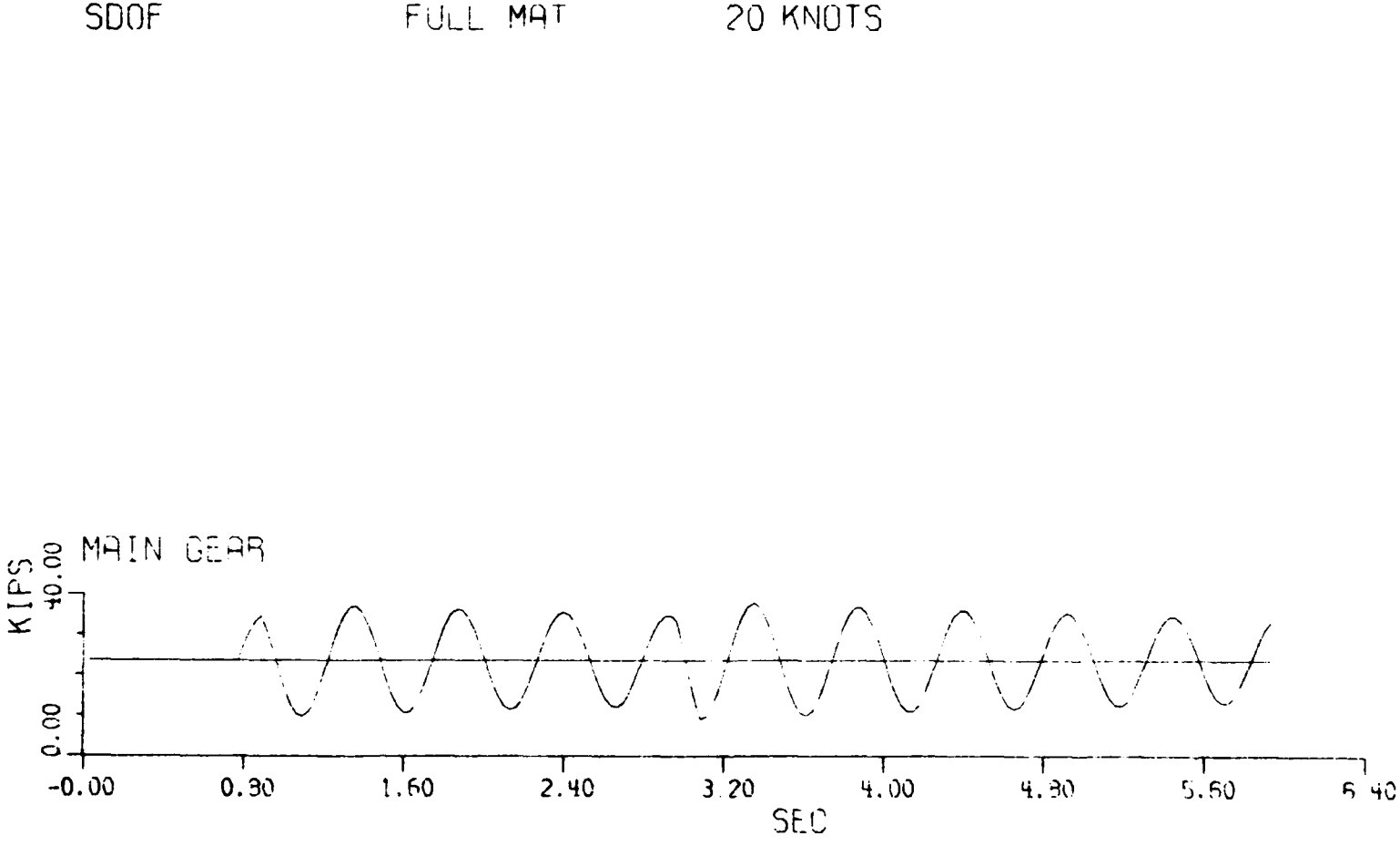

Figure 9. SDOF Code Response to Full Mat Profile

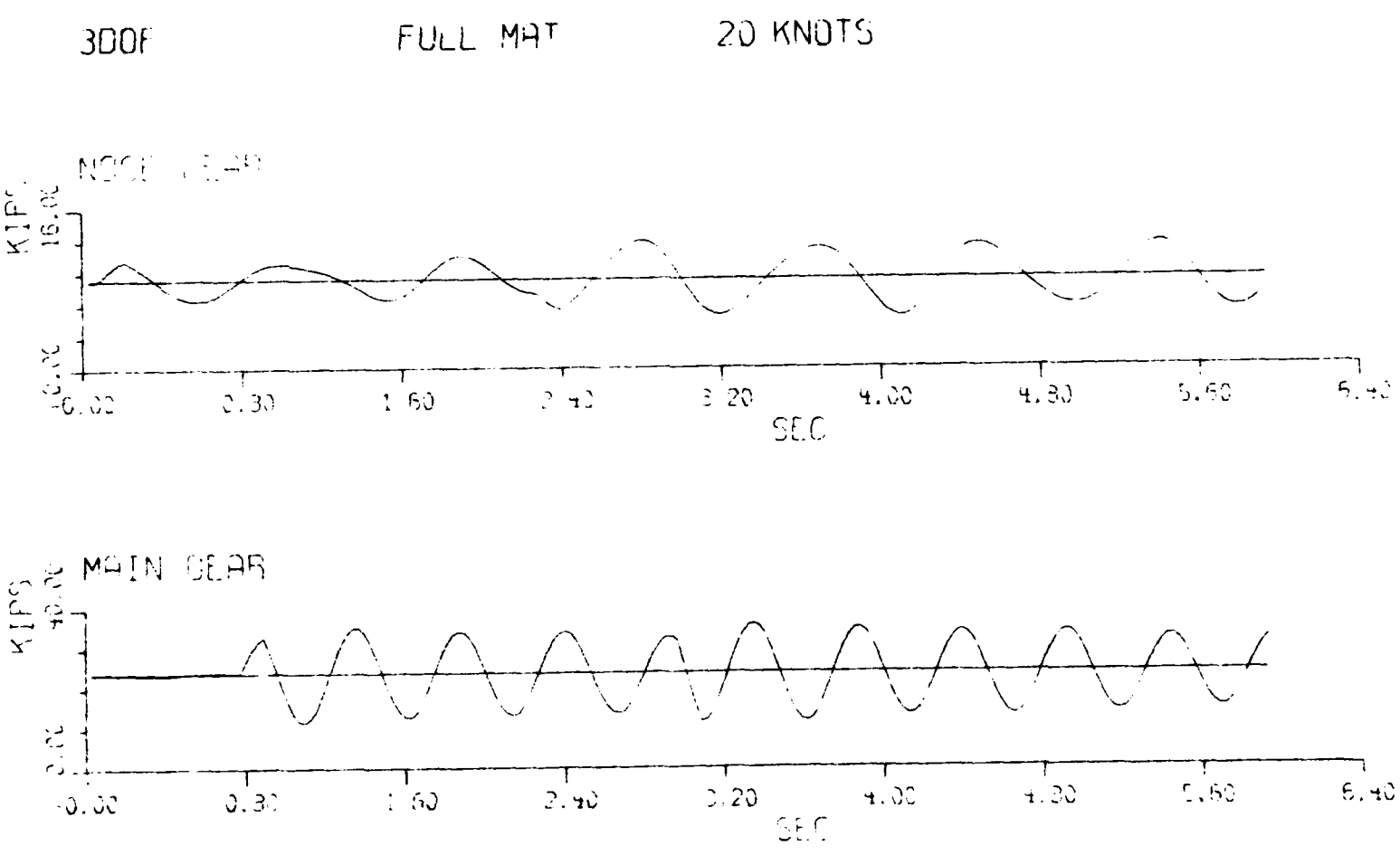

Figure 10. 3DOF Code Response to Full Mat Profile

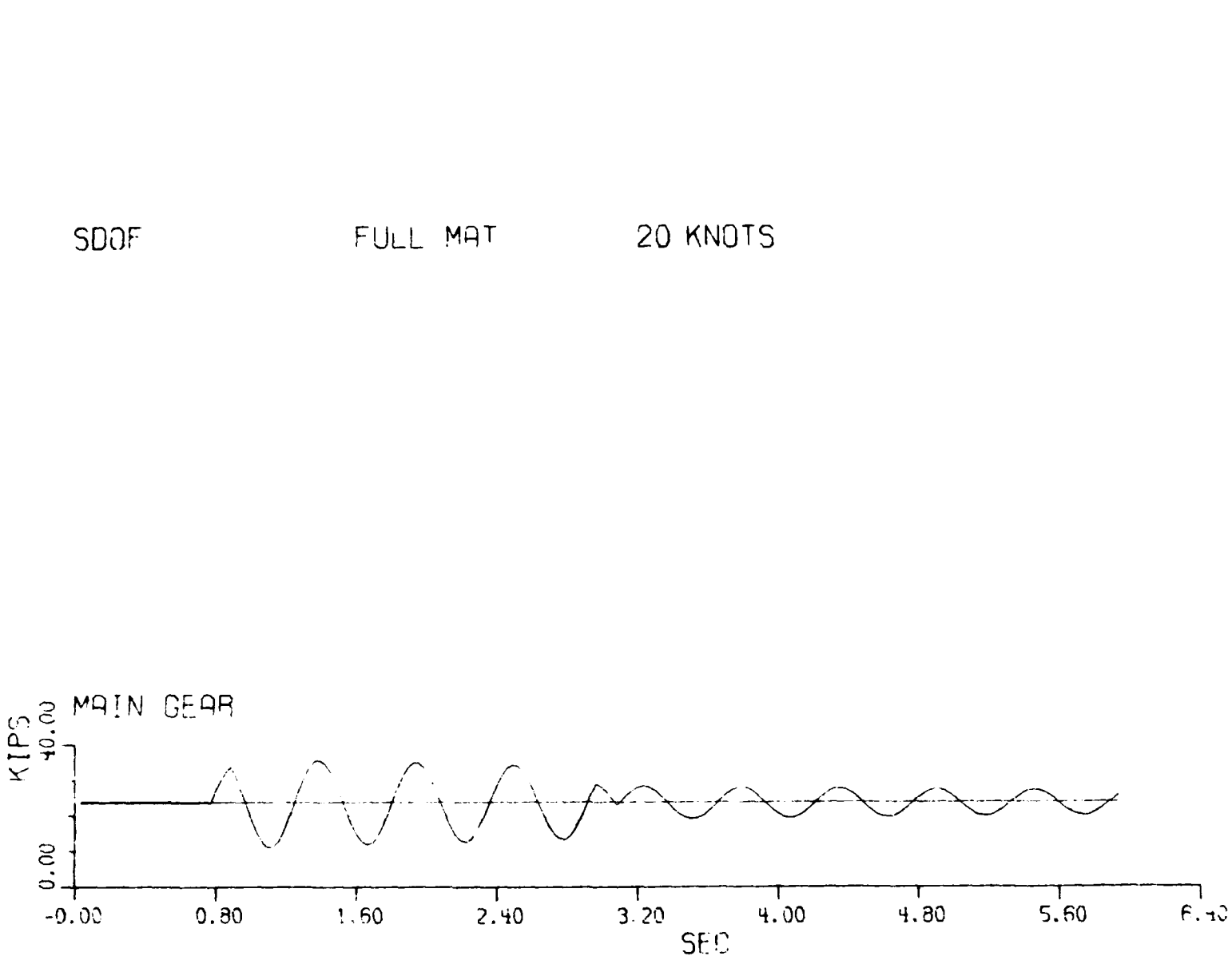

Figure 11. SDOF Code Response with Frequency = 1.80 Hertz

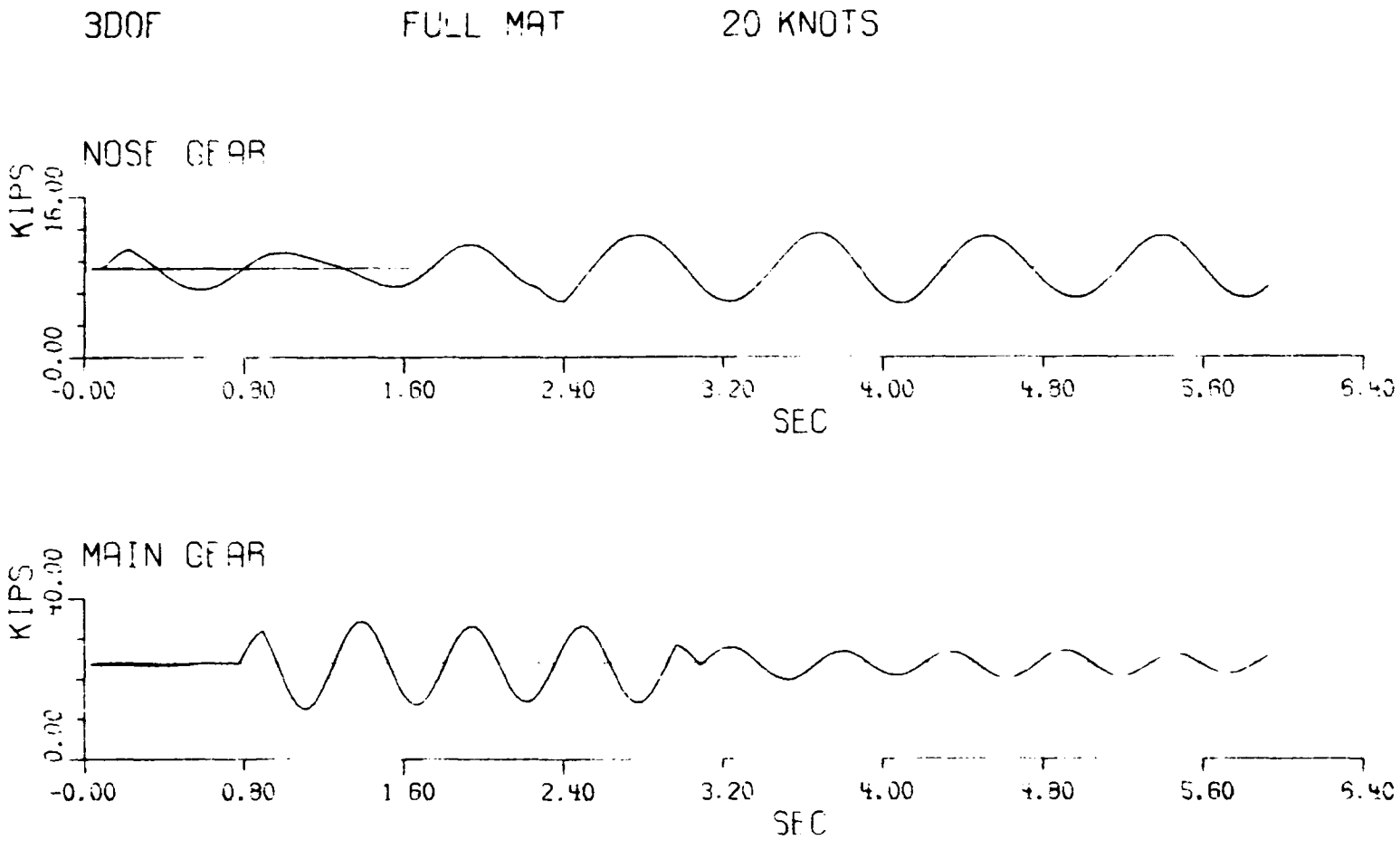

Figure 12. 3DOF Code Response with Modified Spring Constants

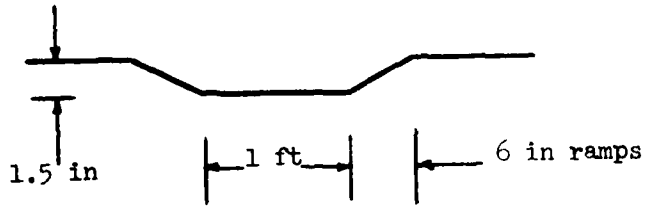

Two-Foot Spall

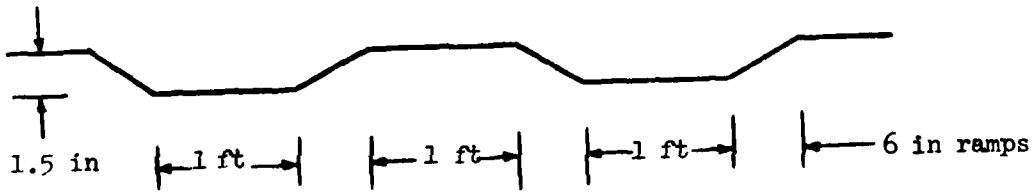

Double Spall

Figure 13. Spall Models

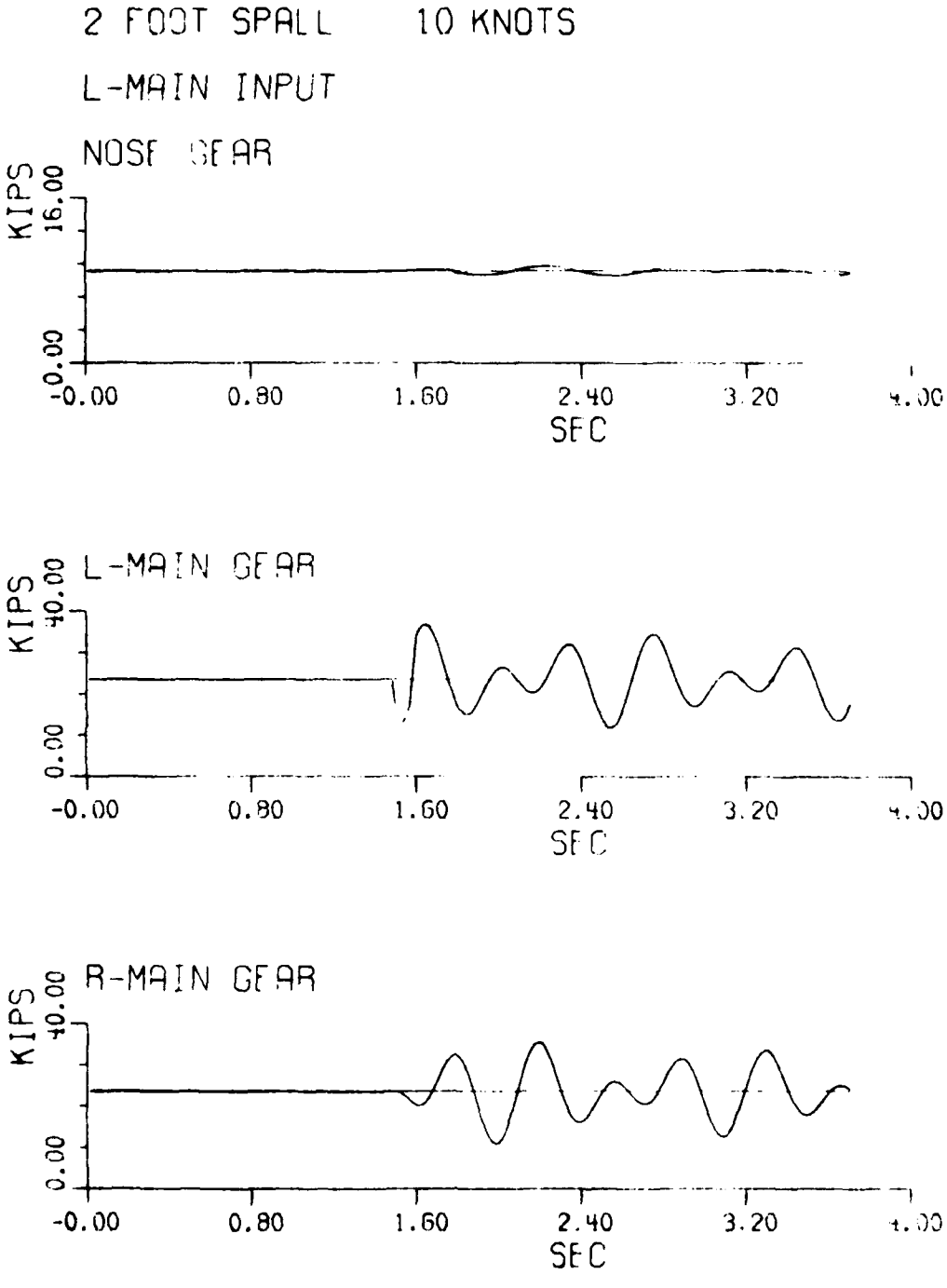

Figure 14. Response to Two-Foot Spall for Left Main Gear Input

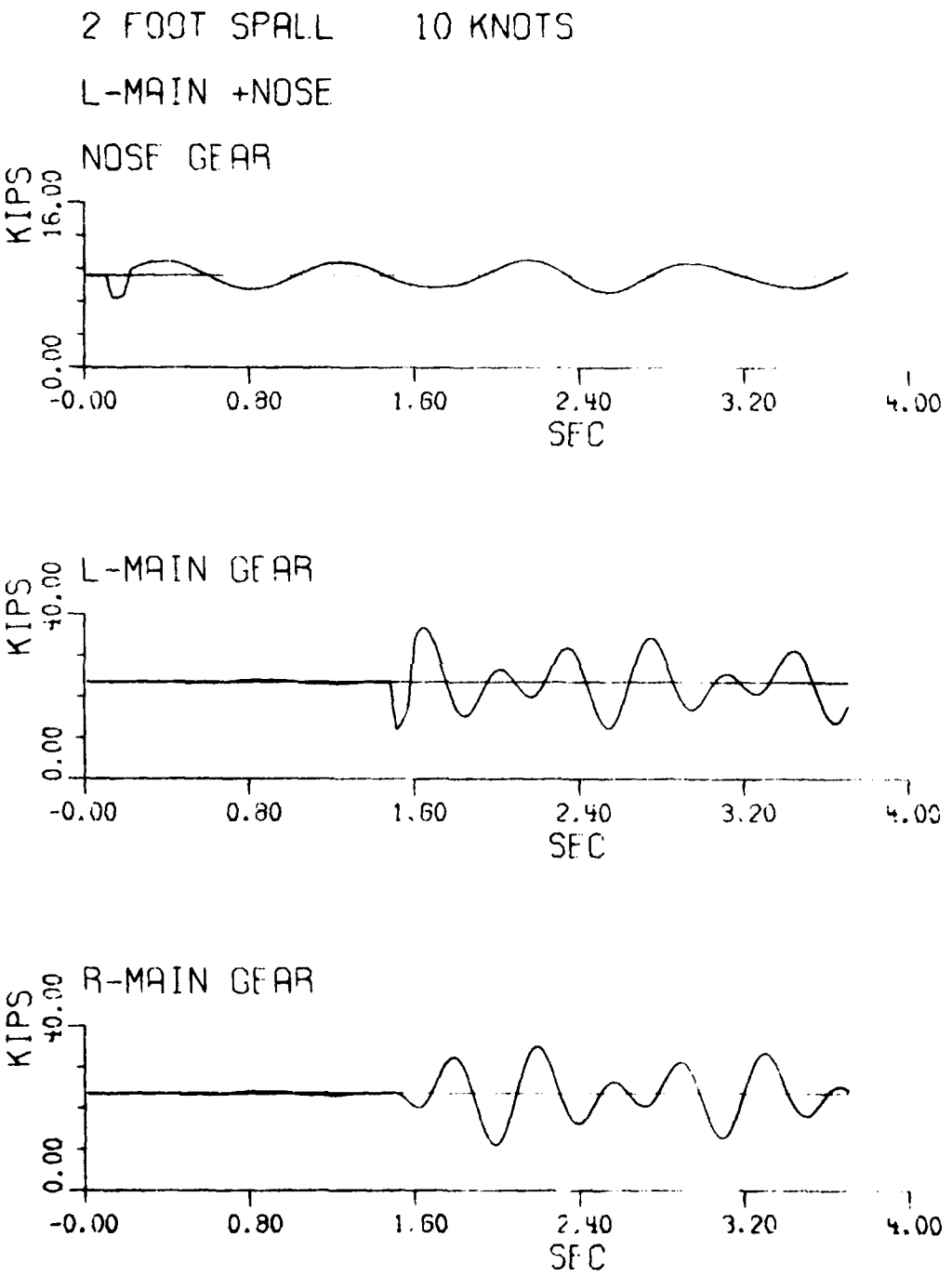

Figure 15. Response to Two-Foot Spall for Left Main and Nose Gear Input

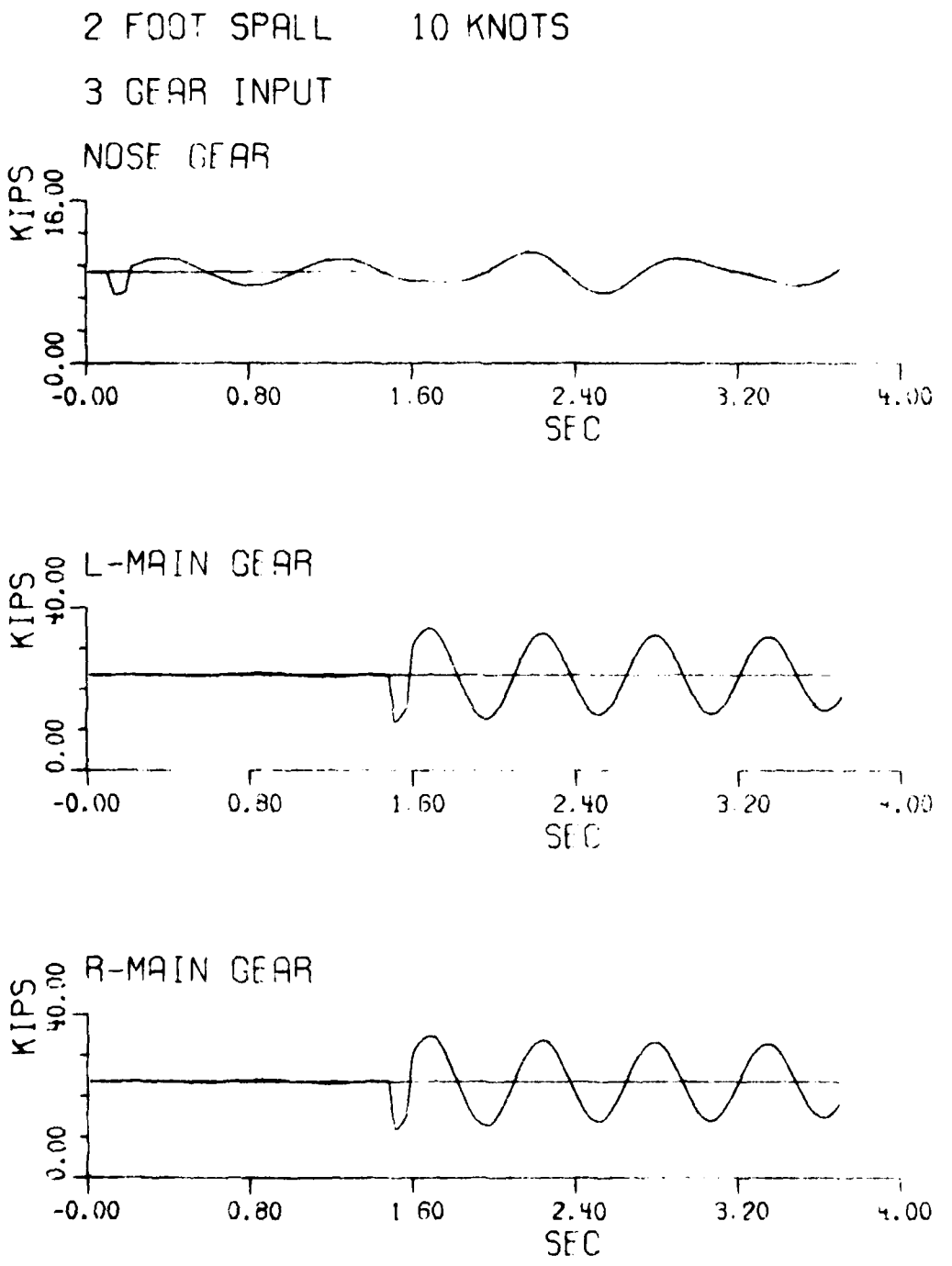

Figure 16. Response to Two-Foot Spall for Three Gear Input

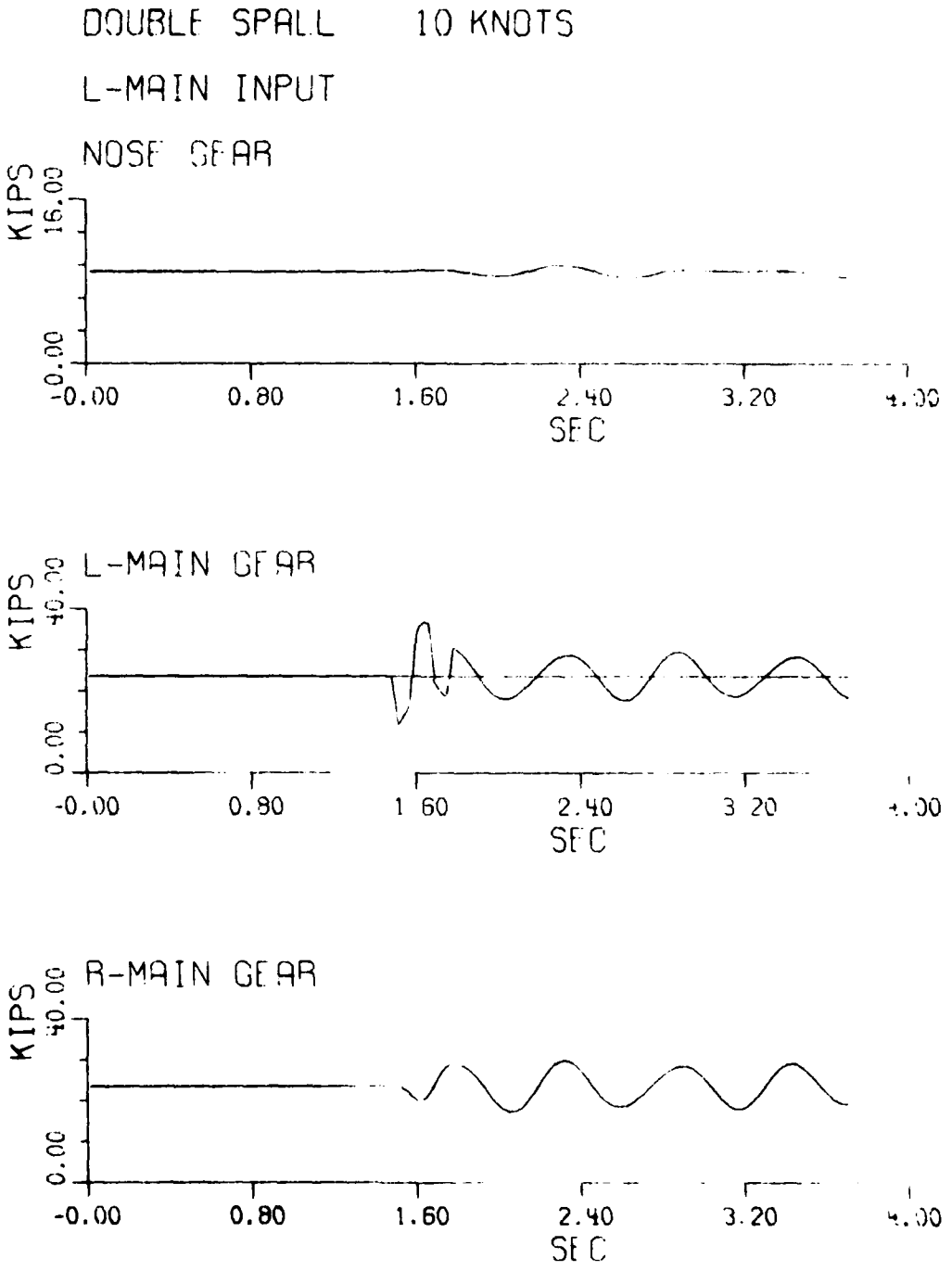

Figure 17. Response to Double Spall for Left Main Gear Input

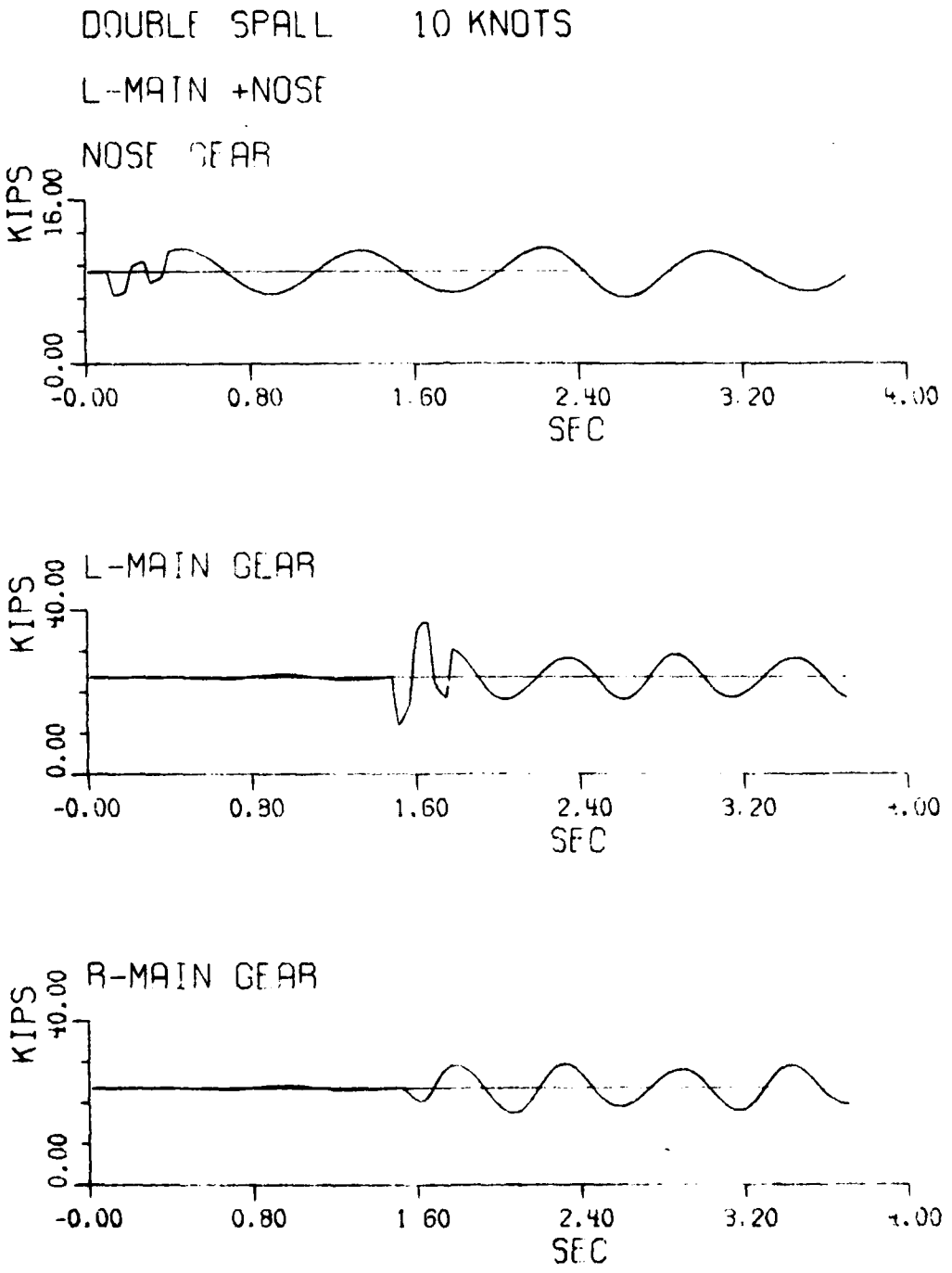

Figure 18. Response to Double Spall for Left Main and Nose Gear Input

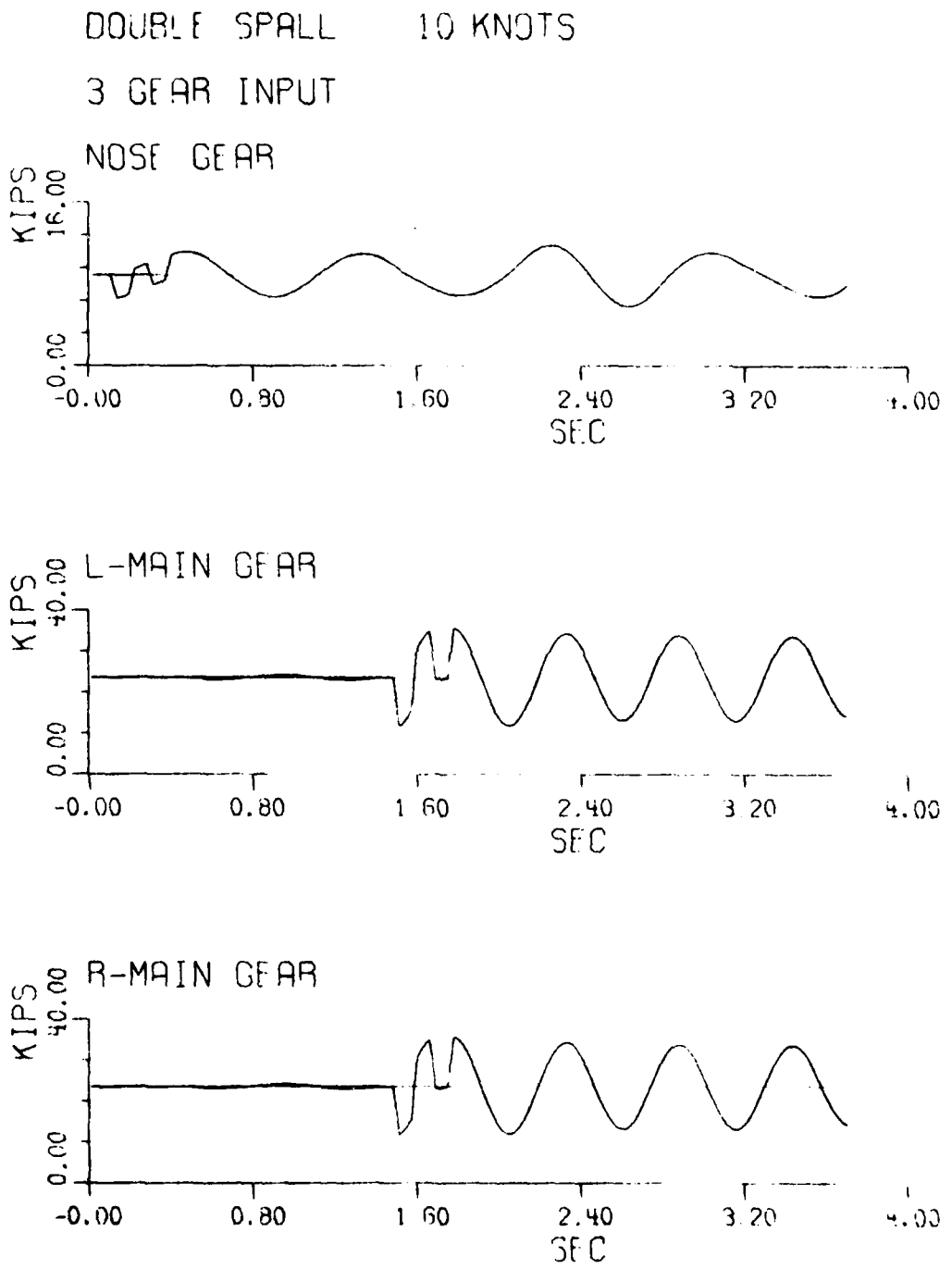

Figure 19. Response to Double Spall for Three Gear Input

SECTION V

CONCLUSIONS AND RECOMMENDATIONS

The one- and three-degree-of-freedom linear vibration models developed in this report can reproduce the response of the essentially nonlinear aircraft system to surface roughness. To correctly reproduce the response to runway mats, it is important that the linear model have spring constants that produce the same period of free vibration so that the phasing of the trailing edge of the mat will cause the same reinforcement and cancellation phenomena.

The three-degree-of-freedom model can accept arbitrary runway profile inputs for each gear. It can be used to predict results of asymmetric motion due to spalls in the runway. The predictions of this model need to be validated using the results of the recent spall tests at the AFFTC.

REFERENCES

1. Program Management Plan for Rapid Runway Repair, AFESC, 31 March 1980.

2. Rapid Runway Repair Procedures, Chapter 5, AFR 93-2, 29 July 1974.

3. Redd, L.T., and Borowski, R.A., HAVE BOUNCE Phase I Test Results, AFFTC-TR-79-1, April 1979.

4. Lenzi, D.C., and Borowski, R.A., HAVE BOUNCE Phase II Test Results, AFFTC-TR-80-4, June 1980.

5. Caldwell, L.R., and Jacobsen, F.J., Interim Guidance for Surface Roughness Criteria, ESL-TR-79-37, October 1979.

6. Wilson, E.L., CAL 78 User Information Manual, Report UC SESM 79-1, Department of Civil Engineering, University of California, Berkeley, November 1978.

7. Gerardi, A.G., and Lohwasser, A.K., Computer Program for the Prediction of Aircraft Response to Runway Roughness, AFWL-TR-73-109, Volume 1, September 1973.

8. Tse, F.S., Morse, I.E., and Hinkle, R.T., Mechanical Vibrations, Theory and Applications, Second Edition, Allyn and Bacon, Inc., 1978.

9. Bathe, K.J., and Wilson, E.L., Numerical Methods in Finite Element Analysis, Prentice-Hall, Inc., 1976.

10. Wilson, E.L., "CAL-A Computer Analysis Language for Teaching Structural Analysis," Computers & Structures, Volume 10, Pergamon Press Ltd, 1979.

(The reverse of this page is blank)

Initial Distribution

HQ AFSC/DLWM	1
HQ AFSC/SDNE	1
HQ USAFE/DEX	1
AFFTC/TEOF	1
AFFTC/ENAE	1
EOARD/LNS	1
HQ PACAF/DEM	1
HQ TAC/DRP	1
HQ TAC/DEM	1
AUL/LSE 71-249	1
HQ SAC/DEM	1
HQ MAC/DEM	1
HQ AFESC/RDCR	10
HQ AFESC/TST	1
HQ USAFA/DFEM	10
USAE WES	4
AFWAL/FIBE	1
AFIT/DET	1
AFIT (Tech Library)	1
ASD/SD30MF	1
TAC ZEIST	1
550 CE CFE HQ	1
DTIC-DDA-2	2
AFATL/DLODL	1

(The reverse of this page is blank.)